Fractal Analysis of Porous Polycrystalline Titania by Adsorption

Baodian Yao,* Ye Zhang, Huazhong Shi, and Lide Zhang

Institute of Solid State Physics, Academia Sinica, P.O. Box 1129,
Hefei 230031, People's Republic of China

Received October 21, 1999. Revised Manuscript Received July 31, 2000

Porous titania gel monoliths with pure anatase, rutile, and their coexistent phases are prepared by the sol−gel method and subsequent heat treatment, respectively. Their apparent surface nanoscale topography and average roughness are studied using atomic force microscopy (AFM). The AFM images show that the porous titania gel monoliths are composed of aggregates of spherical primary particles. These aggregates also form interparticle pores. The pores are interconnected, open to outer ambient conditions, and are the main contributor to their specific surface area. The surface fractal dimensions (d_{SF}) evaluated with the modified form of the Frenkel−Hasley−Hill (FHH) equation instead of the average roughness from AFM are used to characterize the surface irregularity of these porous crystal titania. The results show that the d_{SF} of titania depends on its crystal structure (CS), and for the same CS, the d_{SF} is independent of heat treatment. The surface dimensions measured are approximately 2.441, 2.500, and 2.413 for pure anatase, pure rutile, and their coexistent titania, respectively, thereby indicating that the fractal surfaces of the rutile are slightly more irregular than that of the other titania phases.

Introduction

Surface irregularity has already been well recognized as a crucial factor in phenomena as diverse as adsorption/desorption, diffusion,[1,2] and catalysis,[3,4] and most dynamics of physical/chemical processes that proceed on the surface of materials are impossible to be independent of it. Therefore, it is very important to characterize the surface irregularity of materials quantitatively.

To characterize surface irregularity, surface science has in the past tended to deal with this problem of description of geometrical irregularity by treating irregularity as a deviation from planar surface geometry. However, it is inconvenient to apply this conventional technique to determine the surface irregularity because it depends on a multitude of model-specific parameters which are difficult to access in practice. The concept of fractal dimension (d_{SF}), introduced by Mandelbrot[5] in 1970s, in contrast, has been successfully applied to characterize the surface irregularity of complex surface geometries.

It is well-known that a fractal surface is invariant over a certain range of scale transformations and is self-similar upon changes in resolution. The degree of its irregularity can be given by the value of the d_{SF}, $2 \leq d_{SF} < 3$. The higher the d_{SF} value, the more wiggly and space filling the surface. The fact that the surfaces of most solid substances are fractals[6] makes a fractal approach useful and universal to apply d_{SF} to characterizing material surface irregularity. The methods applied to determine the surface fractal dimension include electronic energy transfer,[7] small-angle X-ray scattering,[8−10] and adsorption.[10−13] Among them, the adsorption method is a relatively simple and widely applied one to determine the d_{SF}.

In a series of adsorption experiments and analyses of relative adsorption data, three types of analyses were employed, which will be called methods 1, 2, and 3, respectively. In method 1, the number of adsorbed molecules in a monolayer expressed as gas volume V_m at standard temperature and pressure (STP) was measured as a function of the cross-sectional area (σ) of the corresponding adsorbate. The value of the d_{SF} can be estimated from the relation:[14,15]

$$\ln(v_m) = (-d_{SF}/2)\ln(\sigma) + \text{constant} \qquad (1)$$

In method 2, for a series of one class of materials with different particle sizes, specific surface area (SSA) is

---

* To whom correspondence should be addressed. Tel: (0551)-5591465. FAX: +86-551-5591434. E-mail: nanolab@mail.issp.ac.cn

(1) Samuel, J.; Ottolenghi, M.; Avnir, D. *J. Phys. Chem.* **1991**, *95*, 1890.

(2) Samuel, J.; Ottolenghi, M.; Avnir, D. *J. Phys. Chem.* **1992**, *96*, 6398.

(3) Gutfraind, R.; Sheintuch, M.; Avnir, D. J. *Chem. Phys.* **1991**, *95*, 6100.

(4) Seri-Levy, A.; Avnir, D. *Surf. Sci.* **1991**, *248*, 258.

(5) Mandelbrot, B. B. *The Fractal Geometry of Nature*; Freeman: San Francisco, CA, 1982.

(6) Avnir, D.; Farin, D.; Pfeifer, P. *Nature* **1984**, *308*, 261.

(7) Rojanski, D.; Huppert, D.; Bale, H. D.; Dacai, X.; Schmidt, P. W.; Farin, D.; Seri-Levy, A.; Avnir, D. *Phys. Rev. Lett.* **1986**, *56*, 2505.

(8) Bale, H. D.; Schmidt, P. W. *Phys. Rev. Lett.* **1984**, *53*, 596.

(9) Cole, M. W.; Holter, N. S.; Pfeifer, P. *Phys. Rev. B* **1986**, *33*, 8806.

(10) Sonwane, C. G.; Bhatia, S. K.; Calos, N. J. *Langmuir* **1999**, *15*, 4603.

(11) Ismail, Ismail M. K.; Pfeifer, P. *Langmuir* **1994**, *10*, 1532.

(12) Meng, F.; Schlup, J. R.; Fan, L. T. *Chem. Mater.* **1997**, *9*, 2459.

(13) Jaroniec, M.; Kruk, M.; Olivier, J. P. *Langmuir* **1999**, *15*, 5410.

(14) Pfeifer, P.; Avnir, D. J. *Chem. Phys.* **1983**, *79*, 3558.

(15) Avnir, D.; Farin, D.; Pfeifer, P. J. *Chem. Phys.* **1983**, *79*, 3566.

10.1021/cm990674c CCC: $19.00

measured as a function of the particle diameter (D) using one adsorbate. The value of the d_{SF} can be determined from the equation:[6,16]

$$\ln(\mathrm{SSA}) = (d_{SF} - 3)\ln(D) + \text{constant} \tag{2}$$

In method 3, the fractal dimension was determined in one step from a single adsorption isotherm utilizing a modified form of the Frenkel−Hasley−Hill (FHH) equation proposed by Avnir et al.[17]

$$\ln(V) = (d_{SF} - 3)\ln(-\ln(P/P_0)) + \text{constant} \tag{3}$$

where V is the adsorbed volume of adsorbate at STP and P/P_0 is the relative pressure. The same equation is also derived by Yin[18] by incorporating a fractal pore size distribution into the Kelvin equation for capillary condensation on porous materials.

Equation 3 indicates that d_{SF} can be obtained from the slope of a log−log plot of the adsorbed volume of adsorbate, V, vs the relative pressure P/P_0. Therefore, method 3 is more convenient and simple than the other two because it does not require knowledge of the values of σ or D. But it should be noticed that eq 3 holds only when the capillary condensation occurs.

Little work has been done so far on the surface fractal dimensions of crystal materials. In the case of titania, to our best knowledge, there is only one report about the fractal dimensions of polymeric and particulate titania aerogels by Meng et al.,[12] and no attention had been paid to the d_{SF} of crystal titania. Considering the fact that titania is widely used in the form of a polycrystal, it is of great significance to investigate the d_{SF} of crystalline titania. In the present work, porous TiO_2 gel monoliths with different phase structures are first prepared by the sol−gel method followed by heat treatment. Their topography and average roughness are obtained from the AFM images, and then their surface fractal dimensions are determined using the FHH method.

Experimental Procedure

Sample Preparation. The porous polycrystalline titania samples used in this study were prepared by hydrolyzing a titania precursor, tetrabutyl titanate, with deionized water catalyzed by acetic acid in a solution of butyl alcohol. Two series of samples, A samples and B samples, were prepared with the molar composition of 1:3:8:3 and 1:3:8:4, respectively, following the order of tetrabutyl titanate/acetic acid/butyl alcohol/water. The typical preparative procedure was as follows. A 20-mL portion of tetrabutyl titanate was first added to a mixture of 10 mL of acetic acid and 43 mL of butyl alcohol to form a solution. After the mixture was stirred for half an hour, the solution was hydrolyzed by adding adequate deionized water (A sample, ∼3.4 mL; B sample, ∼4.5 mL) in the form of ice under furious magnetic stirring at room temperature. After complete homogenization, the sols were cast into glass vessels covered with plastic films having pinholes to gel and age at room temperature. After about 40 days, transparent titania gel monoliths were obtained. These as-prepared TiO_2 gel monoliths then were fired at various temperatures in air; the heating rate for all samples was 10 °C/h. All samples were held at the peak firing temperatures for 2 h.

Sample Characterization. The X-ray diffraction (XRD) powder patterns obtained on a Phillips Pw 1700 X-ray diffractometer using Cu Kα radiation at a scan rate of 0.06° 2θ s^{-1} were used to determine the identity of the phases present.

The topographies of the A and B samples were obtained by using atom force microscopy (AUTOPROBE CP, Park Scientific Instruments); their average roughness was given by the average deviation of data, referenced to the average of the data within the whole topography. It was determined using the standard definition

$$R_{\mathrm{ave}} = \sum_{n=1}^{N} \frac{|Z_n - \bar{Z}|}{N}$$

where $\bar{Z}$ is the mean Z height, N is the the number of data points in the included area.

Nitrogen-gas physisorption measurements for all the samples were conducted at liquid-nitrogen temperature using a Micromeritics ASAP 2000 apparatus. All of the samples were degassed at 110 °C before the actual measurements. The specific surface area and pore size distribution directly were reported by the computer interfaced to the apparatus. The porosity, from the saturation adsorption volume of nitrogen gas obtained from the adsorption branch of the isotherm at STP, was calculated by the relation (the skeleton specific volume of TiO_2 (V_s) is taken as 0.27 and 0.235 cm^3 g^{-1} for anatase and rutile, respectively)

$$P = \frac{V_P}{V_P + V_s} \tag{4}$$

with

$$V_p = (1.547 \times 10^{-3})V_d \tag{5}$$

$$V_s = 0.27(1 - X_R) + 0.235X_R \tag{6}$$

where V_p is the volume of the liquid nitrogen corresponding to the total pore volume, which was calculated from the saturation adsorption volume at STP (V_d) and X_R is the mass fraction of rutile phase in the samples which can be calculated from the equation.[19]

Results and Discussion

Crystal Structure. The as-prepared A sample is anatase (Figure 1). With the calcination temperature increasing up to 600 °C, the intensity of the XRD peaks of anatase increases, but no new phase was observed. The crystal structure of the as-prepared B sample is not a single phase (Figure 2). Anatase and rutile coexist, and the mass fraction of the rutile phase (WFR) is 43.5%. After heat treatment at 500 °C, the WFR of the B sample increases to 63.0%. The B sample becomes a nearly complete rutile structure after heat treatment at 700 °C, as indicated by the nearly complete disappearance of the (101) XRD peak of anatase in Figure 2.

Pore Structure. The full sorption isotherm and pore size distribution diagrams of the as-prepared A sample are shown in Figure 3. This is a typical IV isotherm, indicating that the pores of A samples are mesoporous. The appearance of the hysteresis loop indicates that the pores are interconnected and open to the outer ambient. The same result is obtained for B samples. However, significant differences exist between A and B samples for the values of SSA, porosity, mean pore diameter, and the total pore volume (see Table 1).

---

(16) Avnir, D.; Farin, D.; Pfeifer, P. J. *Colloid Interface Sci.* **1985**, *103*, 112.
(17) Avnir, D.; Jaroniec, M. *Langmuir* **1989**, *5*, 1431.
(18) Yin, Y. B. *Langmuir* **1991**, *7*, 216.
(19) Spurr, P. A.; Myers, H. *Anal. Chem.* **1957**, *29*, 760.

Table 1. Surface Fractal Dimension (d_{SF}), Average Roughness (AR), SSA, Porosity, Mean Pore Diameter, and Total Pore Volume of Titania Samples

sample		d_{SF}	AR (nm)	SSA ($m^2\ g^{-1}$)	porosity (%)	mean pore diameter (nm)	total pore volume (cm^3/g)
A	as-prepared	2.528 ± 0.009	3.3	333	58	4.4	0.37
	300 °C	2.438 ± 0.003	3.9	123	54	10.4	0.32
	400 °C	2.444 ± 0.005	4.0	118	54	10.5	0.31
	500 °C	2.443 ± 0.004	4.1	91	47	10	0.23
	600 °C	2.441 ± 0.003	4.2	25	19	9.8	0.06
B	as-prepared	2.502 ± 0.001	20.0	153	25	3.1	0.08
	500 °C	2.413 ± 0.003	20.9	27	11	3.5	0.03
	700 °C	2.500 ± 0.002	18.3	23	32	21	0.11

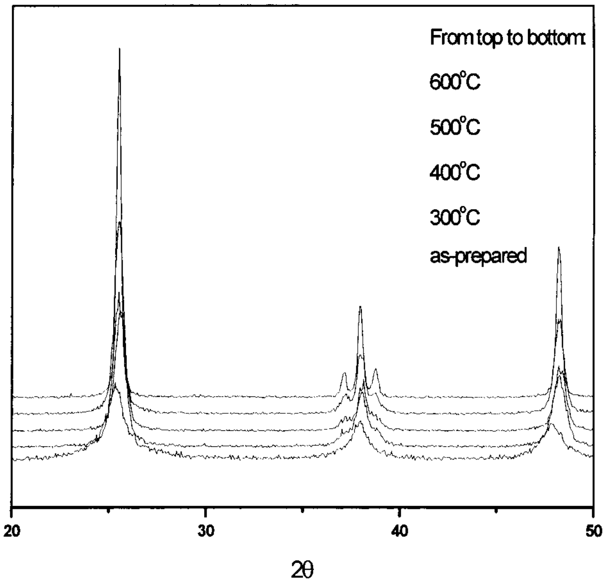

Figure 1. X-ray diffraction patterns of TiO_2 A samples.

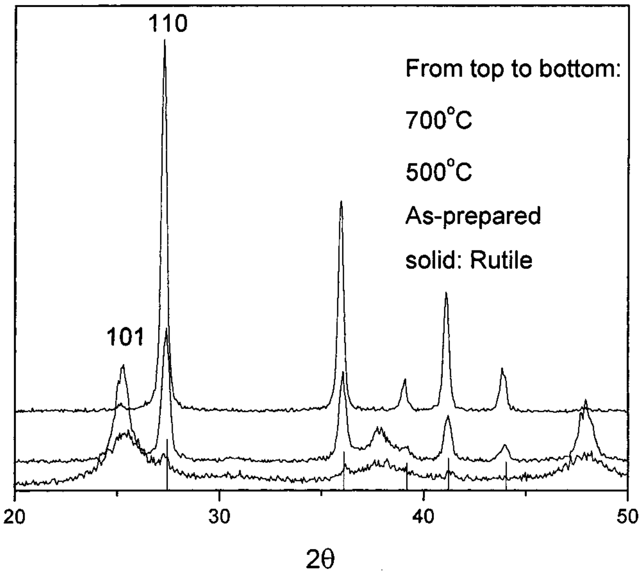

Figure 2. X-ray diffraction patterns of TiO_2 B samples.

Surface Topography and Average Roughness. The AFM images in Figure 4 show clearly that as-prepared A and B samples are composed of aggregates of spherical primary particles. These aggregates pack together to form the gel monoliths and also form interparticle pores. The morphology of these aggregates for A samples evolved from spherelike (Figure 4a) to squarelike (Figure 4b) and then to spherelike (Figure 4c) again, which is concomitant with a slow increase of the surface average roughness, as listed in Table 1.

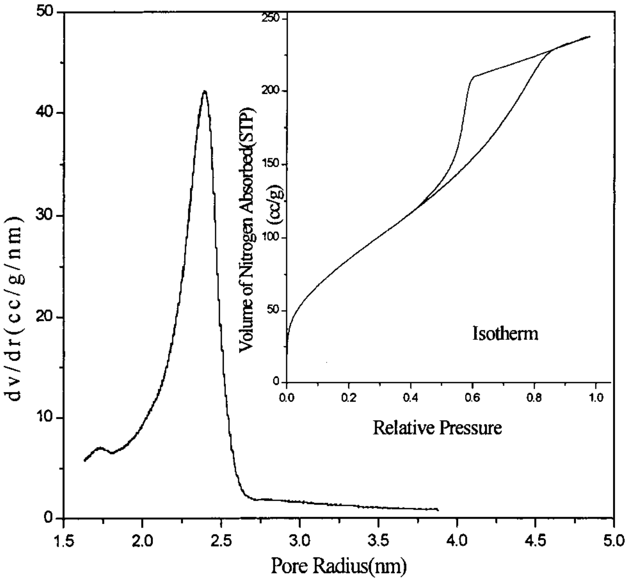

Figure 3. Full sorption isotherm and pore size distribution diagram of TiO_2 as-prepared A sample.

While for B samples, instead of spherelike, the starting morphology of aggregates was nearly squarelike (Figure 4d), and their profile became more clear after heat treatment at 500 °C (Figure 4e). When the heat-treatment temperature increased to 700 °C, that is, when the phase of the B sample was nearly pure rutile, the morphology of aggregates was nearly spherelike (Figure 4f). Compared to A samples (pure anatase phase), the apparent surfaces of B samples are more rough.

Surface Fractal Dimensions. The surface fractal dimensions are used to investigate the whole surface (including outer surface and inner pore walls) irregularity.

According to analysis above and the IUPAC classification,[20] in which the adsorption mechanism occurring in mesopores is capillary condensation, eq 3 is valid in determining the surface fractal dimensions of A and B samples in the present study.

Figure 5 and Figure 6 are the log−log plots of V vs P/P_0 for A and B samples, respectively. The surface fractal dimensions (with error) determined from the slopes of the least-squares fits (to the linear region) are summarized in Table 1. It should be noted here that the start of capillary condensation is dependent on the pore size of samples; the smaller of the pore size, the lower of the relative pressure at which the capillary

---

[20] Greg, S. J.; Sing, K. S. W. *Adsorption, Surface Area and Porosity*; Academic Press: London, 1982.

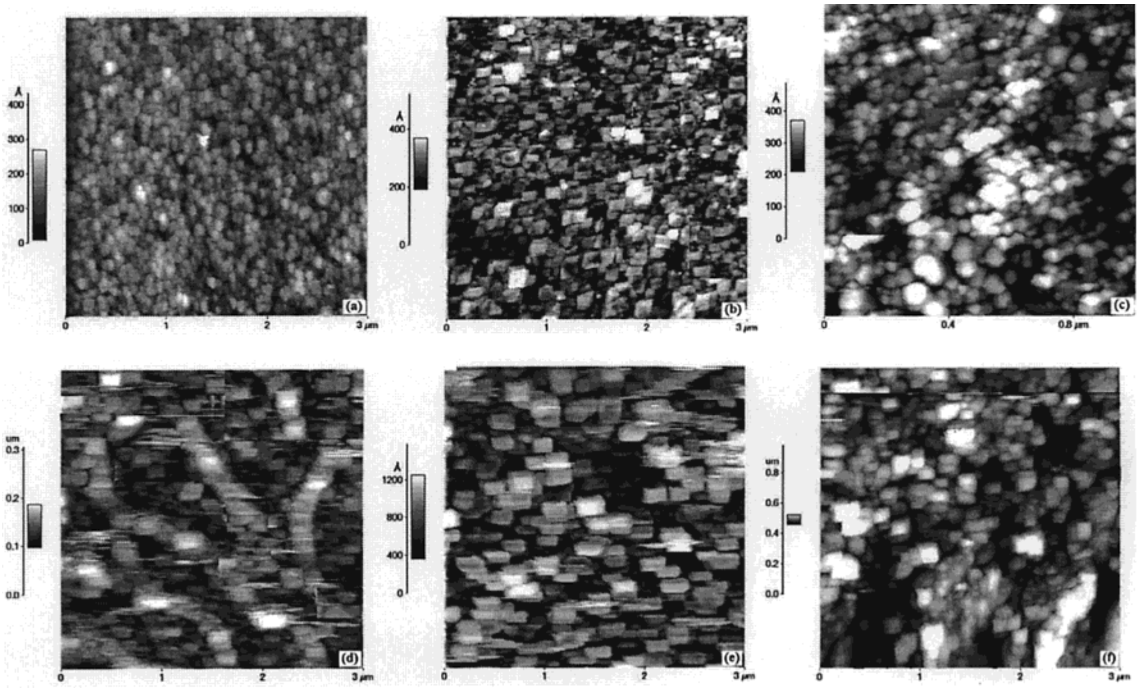

Figure 4. AFM topography of as-prepared (a), 400 °C heat-treated (b), and 600 °C heat-treated (c) A samples and as-prepared (d), 500 °C heat-treated (e), and 700 °C heat-treated (f) B samples. The range of (X, Y) in all figures was 3 μm × 3 μm but 1 μm × 1 μm in panel c. The Z height selected to make the photograph legible was not the same for all samples as indicated by the left legend.

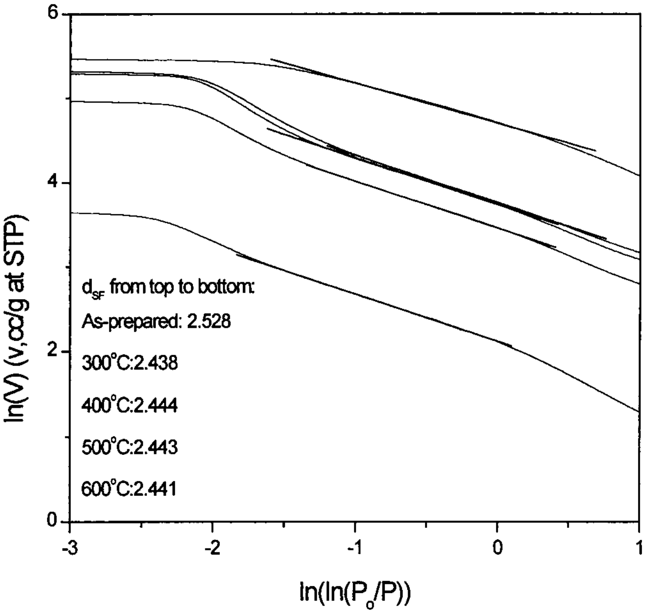

Figure 5. FHH plots for N_2 adsorption on TiO_2 A samples.

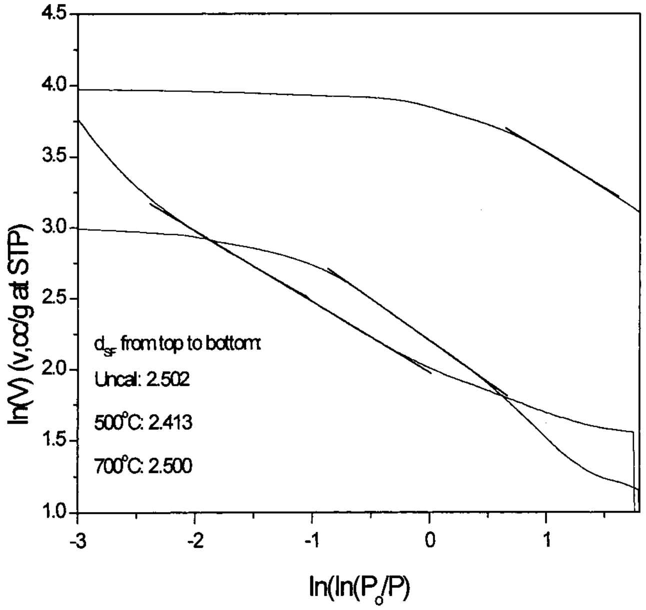

Figure 6. FHH plots for N_2 adsorption on TiO_2 B samples.

condensation begins. Therefore, only a certain range of P/P_0 (in which capillary condensation occurs and eq 3 is valid) can be used to obtain d_{SF}. This range is different for samples with different pore size distributions. That is why different ranges were selected in Figure 5 and Figure 6 to obtain the d_{SF}.

As can be seen from Table 1, the d_{SF} of the as-prepared A sample is greater than that of heat-treated A samples. However, for those heat-treated A samples, their surface fractal dimensions are the same within the experimental error. Therefore, the surface fractal dimensions of titania are independent of heat treatment for the samples having the same crystal structure. The fact that the d_{SF} of the as-prepared A sample is greater than that of heat-treated A samples is likely due to the residual organic components in the as-prepared samples. The same explanation can be used to express the fact that the d_{SF} of as-prepared B sample is greater than that of the heat-treated B sample at 500 °C. However, d_{SF} of the B sample is not independent of heat treatment; as can be seen from Table 1, it is 2.413 and 2.500 for 500 and 700 °C heat treatment, respectively. Because the crystal structure of the B sample is varied with different heat treatment temperatures, the d_{SF} of titania depends on crystal structure. In the present experiment, the surface fractal dimension of rutile titania is slightly higher than that for others, while the d_{SF} of the titania, in which anatase and rutile coexist (B sample heat treated at 500 °C), is the lowest.

Conclusion

Transparent porous titania with different crystal structures were prepared by the sol−gel method. The AFM images show that the porous titania gel monoliths are composed of aggregates of spherical primary particles. The adsorption experiment results show that these as-prepared titania gel monoliths are mesoporous, with interconnecting pores which are open to ambient conditions. Their surface fractal dimensions were calculated with the modified form of the FHH equation. The results showed that d_{SF} of titania is dependent on the crystal structure and independent of heat treatment for the same crystal structure. In the three crystal structures, anatase, rutile, and their coexistence, the d_{SF} of rutile is the highest, indicating the fractal surface of rutile titania is most irregular.

Acknowledgment. We thank the Chinese Climbing Program for support of this research. Dr. Yao is grateful to Professor Zhixiang Chen, Institute of Solid State Physics.

CM990674C